Geophysical Research Letters

RESEARCH LETTER
10.1029/2021GL095404

Surface and Intermediate Water Changes Triggering the Future Collapse of Deep Water Formation in the North Western Mediterranean

Iván M. Parras-Berrocal[1], Rubén Vázquez[1], William Cabos[2], Dimitry V. Sein[3], Oscar Álvarez[1], Miguel Bruno[1], and Alfredo Izquierdo[1]

[1]Instituto Universitario de Investigación Marina (INMAR), Universidad de Cádiz, Puerto Real, Spain, [2]Departmento de Física y Matemáticas, Universidad de Alcalá, Madrid, Spain, [3]Alfred Wegener Institute for Polar and Marine Research, Bremerhaven, Germany

Key Points:

- The North Western Mediterranean deep water formation (DWF) collapse by mid-21st century under the RCP8.5 scenario
- The collapse is mostly driven by changes in the properties of the Modified Atlantic Water and Levantine Intermediate Water
- The DWF collapse is associated to changes in fluxes through the Strait of Gibraltar

Supporting Information:

Supporting Information may be found in the online version of this article.

Correspondence to:

I. M. Parras-Berrocal,
ivan.parras@uca.es

Citation:

Parras-Berrocal, I. M., Vázquez, R., Cabos, W., Sein, D. V., Álvarez, O., Bruno, M., & Izquierdo, A. (2022). Surface and intermediate water changes triggering the future collapse of deep water formation in the North Western Mediterranean. *Geophysical Research Letters*, *49*, e2021GL095404. https://doi.org/10.1029/2021GL095404

Received 1 AUG 2021
Accepted 25 JAN 2022

Author Contributions:

Conceptualization: Iván M. Parras-Berrocal, Rubén Vázquez, William Cabos, Oscar Álvarez, Miguel Bruno, Alfredo Izquierdo
Data curation: Iván M. Parras-Berrocal, Alfredo Izquierdo
Formal analysis: Iván M. Parras-Berrocal, Alfredo Izquierdo
Funding acquisition: Oscar Álvarez
Investigation: Iván M. Parras-Berrocal, Rubén Vázquez, William Cabos, Alfredo Izquierdo

Abstract Deep water formation (DWF) in the North Western Mediterranean (NWMed) is a key feature of Mediterranean overturning circulation. DWF changes under global warming may have an impact on the Mediterranean biogeochemistry and marine ecosystem. Here we analyze the deep convection in the Gulf of Lions (GoL) in a changing climate using a regional climate system model with a horizontal resolution high enough to represent DWF. We find that under the RCP8.5 scenario the NWMed DWF collapses by 2040–2050, leading to a 92% shoaling in the winter mixed layer by the end of the century. The collapse is related to a strengthening of the vertical stratification in the GoL caused by changes in properties of Modified Atlantic Water and Levantine Intermediate Water, being their relative contribution to the increase of the stratification 57.8% and 42.2%, respectively. The stratification changes also alter the Mediterranean overturning circulation and the exchange with the Atlantic.

Plain Language Summary The deep water formation (DWF) that takes place in the North Western Mediterranean is one of the main drivers of the Mediterranean circulation. Earth's climate warming may affect the DWF, which could trigger large impacts on the Mediterranean ecosystems. This study analyzes the effect of climate change on the DWF in the Gulf of Lions using a Regional Climate System Model. We find out that under a high greenhouse gasses emission scenario the DWF in the North Western Mediterranean collapses by mid-21st century. The collapse is mostly driven by changes in the temperature and salinity of surface and intermediate waters, which increases the stratification in the water column, hampering the deep convection. This DWF collapse in the Gulf of Lions reflects on the flows exchanged between the Atlantic Ocean and the Mediterranean Sea through the Strait of Gibraltar, which evidence changes in the Mediterranean circulation.

1. Introduction

The Mediterranean Sea is a semi-enclosed basin where evaporation exceeds precipitation and river run-off causing a deficit in the freshwater balance that is compensated by a net water transport through the Strait of Gibraltar (SoG; Béthoux & Gentili, 1999; Millot, 1999; Robinson et al., 2001; Sánchez-Gómez et al., 2011). Atlantic Water (AW) flows through the western and into the eastern basin increasing its density and forming the Modified Atlantic Water (MAW). In winter, the oceanic conditions and the intense local air–sea interactions lead to convection of MAW in the Levantine basin producing the Levantine Intermediate Water (LIW; Millot, 2014). The LIW spreads westward at 150–600 m flowing through the Sicily strait and into the Tyrrhenian Sea, reaching the northwestern Mediterranean approximately a decade after its formation (Millot, 2005). The LIW contributes to the Mediterranean outflow to the Atlantic Ocean, forming the main thermohaline circulation cell of the Mediterranean (Lascaratos et al., 1993; Robinson et al., 2001; Vargas-Yáñez et al., 2012). Winter deep convection also takes place in the Northwestern Mediterranean Sea (NWMed; Durrieu de Madron et al., 2013; Marshall & Schott, 1999; MEDOC-MEDOC Group, 1970), triggered by cold and dry regional winds of Mistral (northwesterly) and Tramontane (northerly; Leaman & Schott, 1991; Somot et al., 2018). These winds episodes induce intense surface buoyancy loss associated to a rapid surface cooling and strong evaporation (Schott & Leaman, 1991; Seyfried et al., 2017). In the Gulf of Lions (GoL), the regional cyclonic circulation of MAW and of the underlying LIW (warmer and saltier) drives a doming of isopycnals that reduces the stratification locally and favors deep convection (Houpert et al., 2016; Rhein, 1995). The doming of isopycnals and the large surface buoyancy loss

Methodology: Iván M. Parras-Berrocal, William Cabos, Dimitry V. Sein, Alfredo Izquierdo
Project Administration: Oscar Álvarez, Miguel Bruno
Resources: William Cabos, Dimitry V. Sein, Miguel Bruno, Alfredo Izquierdo
Supervision: William Cabos, Alfredo Izquierdo
Visualization: Iván M. Parras-Berrocal, Rubén Vázquez
Writing – original draft: Iván M. Parras-Berrocal, Alfredo Izquierdo
Writing – review & editing: Iván M. Parras-Berrocal, William Cabos, Dimitry V. Sein, Oscar Álvarez, Alfredo Izquierdo

contribute to the deepening of the convection layer and to the formation of the Western Mediterranean Deep Water (WMDW). The WMDW formation is commonly described in three phases (Marshall & Schott, 1999; Waldman et al., 2017): The preconditioning phase, the intense mixing phase and the restratification-spreading phase.

Waldman et al. (2018) also point out that the intrinsic ocean variability, related to baroclinic instability of the cyclonic gyre, could determinate the occurrence or not of deep convection, especially at interannual time scale.

The NWMed deep water formation (DWF), which takes place mainly in the GoL and in the Ligurian Sea (Margirier et al., 2020), may be affected by the warmer and dryer conditions expected by 2100 under IPCC scenarios (Darmaraki et al., 2019; IPCC, 2013; Soto-Navarro et al., 2020). In fact, the Mediterranean region is considered a "hot spot" climate change region (Giorgi, 2006), where the mean SST is projected to increase from 0.5°C to 3.1°C (e.g., Adloff et al., 2015; Darmaraki et al., 2019; Parras-Berrocal et al., 2020; Somot et al., 2006, 2008; Soto-Navarro et al., 2020) by the end of the century. The warming could increase the stratification and thus reduce the deep convection (Somot et al., 2006), which is essential in sustaining the Mediterranean overturning circulation.

In the GoL, winter deep convection exhibits a strong interannual variability. The mixed layer depth (MLD) is shallow in summer due to surface warming; while in late winter the MLD can be deeper than 800–1,000 m (D'Ortenzio et al., 2005; Somot et al., 2018).

The NWMed DWF has been largely studied (Durrieu de Madron et al., 2013; Estournel et al., 2016; Houpert et al., 2016; Leaman & Schott, 1991; Margirier et al., 2020; MEDOC-MEDOC Group, 1970; Testor et al., 2018) and many attempts to characterize DWF events in the NWMed using high temporal and spatial resolution numerical models have been made (Léger et al., 2016; Seyfried et al., 2017; Somot et al., 2018; Waldman et al., 2017). Most of these works are focused on the impact of atmospheric forcing and ocean preconditioning on the deep convection. Margirier et al. (2020) found, using glider observations, that an increase in LIW temperature (0.3°C) and salinity (0.08) limits the winter mixing, blocking the export of heat and salt to deeper layers. An analysis of the yearly maximum MLD in downscaled climate simulations (Soto-Navarro et al., 2020) suggests a strong reduction in the intensity of DWF that is especially noticeable in the GoL, where the maximum MLD decreases from the present range of 334–2167 m to 209–798 m under RCP8.5 by the end of the 21st century. Several studies have analyzed future climate change projections at regional scales but only few of them investigate the DWF response to climate change, pointing to a strong reduction of deep convection (Adloff et al., 2015; Somot et al., 2006; Soto-Navarro et al., 2020). However, the causes of the reduction remain unexplored.

To tackle this issue, a climate change projection under the RCP8.5 scenario is dynamically downscaled with a regionally coupled model. The model has demonstrated good skills reproducing the present climate in the NWMed region (Parras-Berrocal et al., 2020) including the DWF at GoL (Text S1 in Supporting Information S1) and it has been employed to study future climate (Darmaraki et al., 2019). Moreover, it is a member (AWI25-MPI-8.5) of the ensemble used in Soto-Navarro et al. (2020), showing the strong reduction of DWF intensity reported there. Based on these premises, the objectives of this work are:

1. To quantify the projected reduction of NWMed DWF in ROM regional climate system model (RCSM)
2. To identify the mechanisms leading to that reduction
3. To assess its impact on the change of the Mediterranean outflow properties into the Atlantic

The regional coupled system and the experiments used in this work are described in Section 2. Section 3 presents the results for the intensity of DWF, the contribution of atmospheric and hydrographic changes and the fluxes through the SoG. Finally, Section 4 contains the discussion and conclusions.

2. Description of RCSM: ROM

We use the RCSM ROM (REMO-OASIS-MPIOM) developed by Sein et al. (2015). ROM comprises the REgional atmosphere MOdel (REMO; Jacob, 2001), the Max Planck Institute Ocean Model (MPIOM; Jungclaus et al., 2013; Marsland et al., 2003), the HAMburg Ocean Carbon Cycle model (Maier-Reimer et al., 2005), the Hydrological Discharge model (Hagemann & Dümenil-Gates, 1998, 2001), a soil model (Rechid & Jacob, 2006) and a dynamic/thermodynamic sea ice model (Hibler, 1979). The atmosphere and the ocean are coupled via OASIS3 (Valcke, 2013) coupler, while the other sub-models are treated as modules either of the atmosphere or

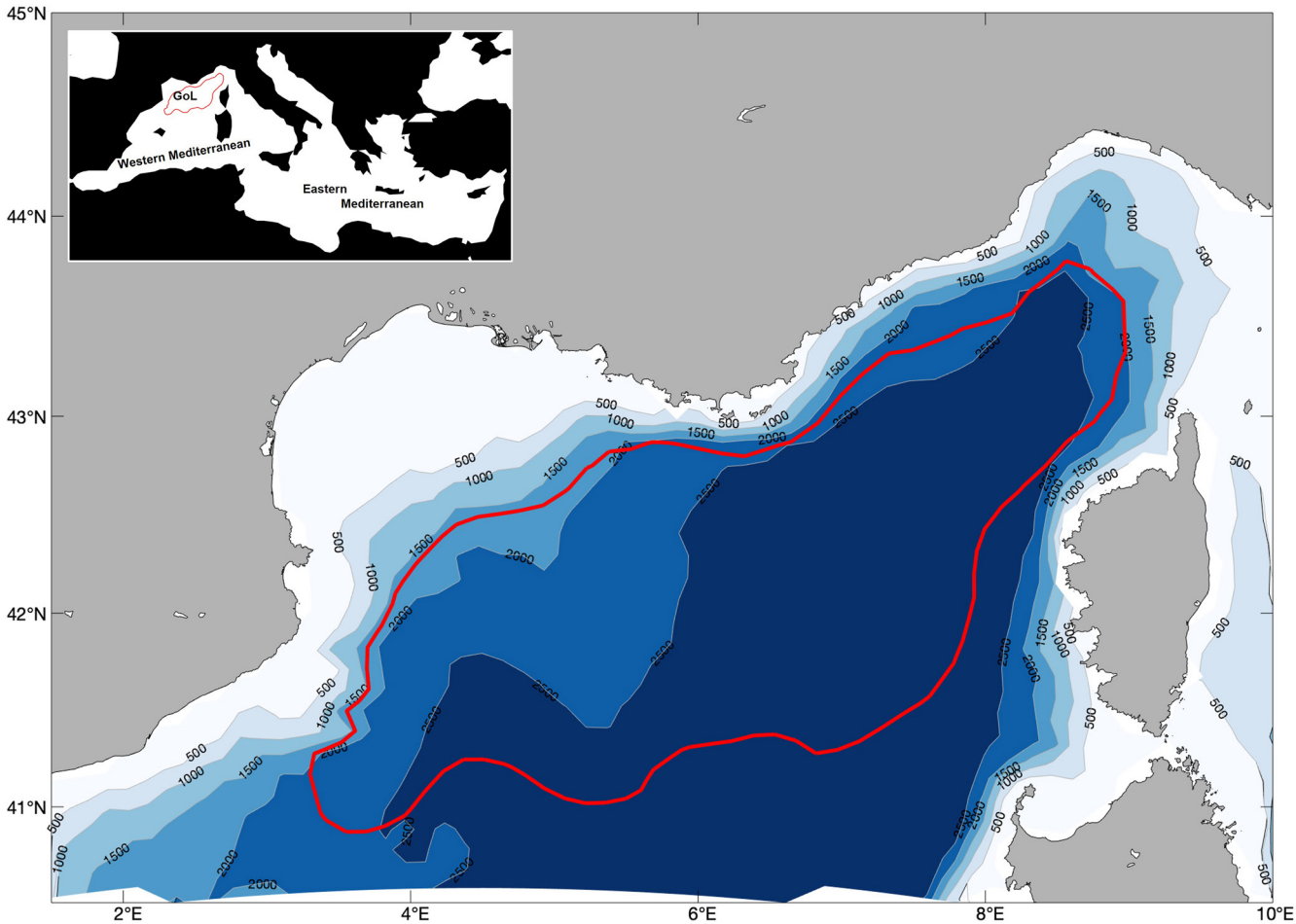

Figure 1. The area representative of the Gulf of Lions deep water formation used in this study is surrounded by the red line; ocean model bathymetry (m) is also shown.

the ocean. The model parameterizations and setup used here are described in Parras-Berrocal et al. (2020) who provide a detailed assessment of ROM-simulated present climate and future changes in the Mediterranean.

MPIOM is formulated on an orthogonal curvilinear Arakawa C-grid with a variable horizontal resolution of 7 km (south Alboran Sea) to 25 km (eastern Levantine Sea) in the Mediterranean with 12 km at GoL, and 40 z-levels with increasing layer thickness with depth (Parras-Berrocal et al., 2020). In MPIOM the water exchange at Gibraltar is not parametrized and the properties of the Atlantic waters are not relaxed toward climatological values. The model simulates explicitly the water exchange through the SoG, allowing propagating the signals from North Atlantic into the Mediterranean Sea, and vice-versa. The spin-up of MPIOM was done according to Sein et al. (2015). First, MPIOM runs in stand-alone mode starting with climatological temperature and salinity data (Levitus et al., 1998). Subsequently, it is integrated four times through the 1958–2002 period forced by ERA-40. For the coupled runs, the model starts from the final state reached in the last stand-alone run and integrated again, forced two times by ERA-40 and one time by ERA-Interim reanalysis (1979–2012). Then, it runs for 56 years (1950–2005) starting from the last state of the coupled simulation forced by ERA-Interim.

In this work, we use 1976–2005 (ROM_P1) as the historical reference period to define the DWF target area in the GoL (Figure 1), and we aim to offer an integrated vision of the impact of climate change on the NWMed DWF under the RCP8.5 for 2006–2099 (ROM_P2). Both simulations are part of the Med-CORDEX initiative (www.medcordex.eu).

As representative of the GoL we use the mixed patch area surrounded by the red line in Figure 1. Somot et al. (2018) have verified that their results are not very sensitive to the choice of the GoL domain if the continental shelf is

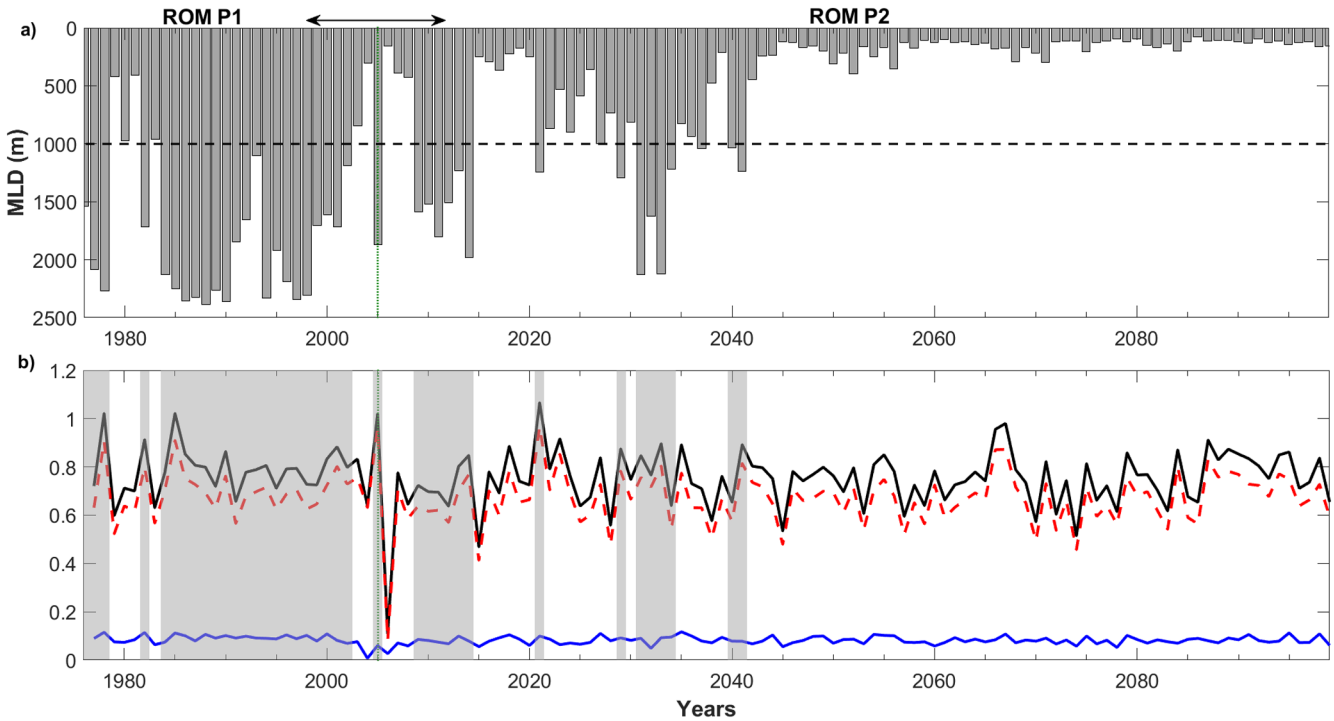

Figure 2. Time series (1976–2099) of ROM_P1 and ROM_P2 simulations of (a) yearly MLD_{max} (m) and (b) winter integrated buoyancy loss (BL) (m^2s^{-2}) averaged over the Gulf of Lions. The black line corresponds to the total BL, the red dashed and the blue lines are the heat-related and the freshwater-related terms, respectively. Gray bars indicate Deep water formation episodes (MLD_{max} > 1000 m).

avoided and the region where open-sea deep convection occurs is included. The selection of the DWF target area was performed using the mean winter MLD for the 1976–2005 period. The mixed patch area is composed by the grid points where the mean winter MLD is deeper than 1000 m, which corresponds to the depth of WMDW prior to the convection (Waldman et al., 2017).

3. Results

3.1. Intensity of GoL Deep Water Convection

The model MLD is defined as the depth, where the density (ρ) increases by 0.125 kg m^{-3} compared to the value in the surface box (Wetzel et al., 2004). ROM is able to reproduce the DWF in NWMed during the present period (1980–2012, Text S1 in Supporting Information S1): ROM simulates deep convection in the 75% of the years, and in 72% according to observational records (Béthoux et al., 2002; Houpert et al., 2016; Mertens & Schott, 1998; Somot et al., 2018).

It is evident a strong reduction of yearly maximum MLD (MLD_{max}) over the GoL by mid-21st century under RCP8.5 emission scenario (Figure 2a). The MLD_{max} for 1976–2005 is 1712 ± 650 m while for 2070–2099 under the RCP8.5 scenario is 137 ± 45 m. That is, the MLD_{max} simulated by ROM experiences a reduction of 92% in the GoL. Soto-Navarro et al. (2020) reported similar values. During 2006–2099, the model projects 15 events of deep convection, defined as a MLD_{max} deeper than 1000 m (Herrmann et al., 2010; Somot et al., 2018), with six episodes occurring in consecutive years between 2009 and 2014 (Figure 2a). These events always correspond to winter (February-March) when the intense mixing phase is activated.

Our results show a collapse of newly formed WMDW (starting from the 2040–2050 decade no convection is simulated), characterized by MLD_{max} shallower than 500 m (Figure 2a). This result holds independently of the criterion used for MLD definition (Figure S2 in Supporting Information S1). Further, we analyze the causes of this collapse.

3.2. Contribution of Changes in the Winter Surface Buoyancy Loss

The role of the winter air-sea fluxes in the MLD_{max} variability is assessed with the accumulated surface buoyancy loss (BL, Equation 2), defined as the time integral of the buoyancy flux (BF, Equation 1). The BF is calculated in terms of heat and freshwater fluxes (Marshall & Schott, 1999; Somot et al., 2018):

$$BF = g \cdot \left(\frac{\alpha \cdot Q_{net}}{\rho_0 \cdot C_p} + \beta \cdot SSS \cdot FWF \right) \quad (1)$$

$$BL(Y) = - \int_{T_1}^{T_2} BF \cdot dt \quad (2)$$

where Q_{net} and FWF are the net surface heat and freshwater fluxes, respectively (both positive downward), g is the gravitational acceleration (9.81 ms^{-2}), α and β the thermal expansion and haline contraction coefficients (respectively calculated as a function of surface T and S), ρ_0 the reference density of sea water 1025 kgm^{-3}, C_p the specific heat capacity of sea water (equal to 4,000 $Jkg^{-1}°K^{-1}$) and SSS the sea surface salinity. Following Somot et al. (2018), the winter accumulated BL (Equation 2) was computed for every year (Y) of the 1976–2099 from December of the previous year (T_1) to March (T_2) and averaged over the GoL (red contour in Figure 1).

The BL over the GoL does not show a significant trend during 1976–2099 and has a mean value of 0.76 ± 0.12 m^2s^{-2}. The BL is widely dominated by the heat-related term (mean value of 0.67 ± 0.11 m^2s^{-2}). The time series of yearly BL and the heat contribution are well correlated ($r = 0.99$) and of the same order of magnitude, while the freshwater term is one order of magnitude smaller and its Pearson correlation coefficient with the BL is 0.61. Our RCP8.5 simulation shows episodes of MLD_{max} deeper than 1000 m only when the BL is over 0.63 m^2s^{-2}. Although the simulated stronger convective episodes (2014, 2031, 2033) show a BL from 0.84 to 0.90 m^2s^{-2}, there are years with MLD_{max} < 200 m (2066, 2067, 2087), with BL > 0.90 m^2s^{-2}. This indicates that the BL is not the only factor determining the intensity of the deep water convection, so factors such as ocean preconditioning could also contribute to the DWF (Margirier et al., 2020).

3.3. Contribution of Hydrographic Changes in the Water Column

To analyze the pre-winter stratification of the water column we have calculated the stratification index (SI) using December data; lower values of SI correspond to a less stratified water column. The SI has been previously employed in multiple Mediterranean studies (L'Hévéder et al., 2013; Margirier et al., 2020; Somot et al., 2018) and is defined as (Turner, 1973).

$$SI = \int_0^h N^2 \, z dz \quad (3)$$

Where N is the Brunt-Väisälä frequency ($N^2 = g/\rho_0 \, \partial_\rho/\partial_z$), z is the depth, ρ the potential density and h the maximum depth of integration which we have chosen to be 1000 m.

Under the RCP8.5 scenario, temperature increases through the whole water column (Figure 3a). The detected warming that originally takes place at the surface is transferred progressively to deeper layers (Parras-Berrocal et al., 2020). In the upper layer (0–150 m) the temperature experiences a warming of 2.7°C, while intermediate (150–600 m) and 600–1000 m layers warm by 2.4°C and 0.9°C (Figure 3b), respectively. By the end of 21st century, the MAW flowing in the upper layer of the GoL is projected to slightly freshen (−0.01 psu) while the intermediate (0.4 psu) and 600–1000 m layers (0.3 psu) tend to get saltier (Figures 3c and 3d). The expected increase in temperature and salinity accelerates from 2040 at 150–600 m (Figures 3b and 3d). The 150–600 m depth range corresponds to the equilibrium depth of LIW (Menna & Poulain, 2010) in the western Mediterranean.

The evolution of mean winter salinities (Figure 3d) shows a different behavior throughout the water column, showing a slightly freshening trend in MAW and a notable salinization in LIW and the 600–1000 m layer (Table S1 in Supporting Information S1).

The pre-winter SI at 1000 m depth shows values close to minimum before the projected DWF events (Figure 3e), which suggests a weaker stratification of the water column. For the 1976–2099 period the SI has a mean value of 1.04 ± 0.53 m^2s^{-2}. Until 2040s the SI shows a slight growth trend ($5.1 \cdot 10^{-3}$ $m^2s^{-2}y^{-1}$). From 2040 on, the

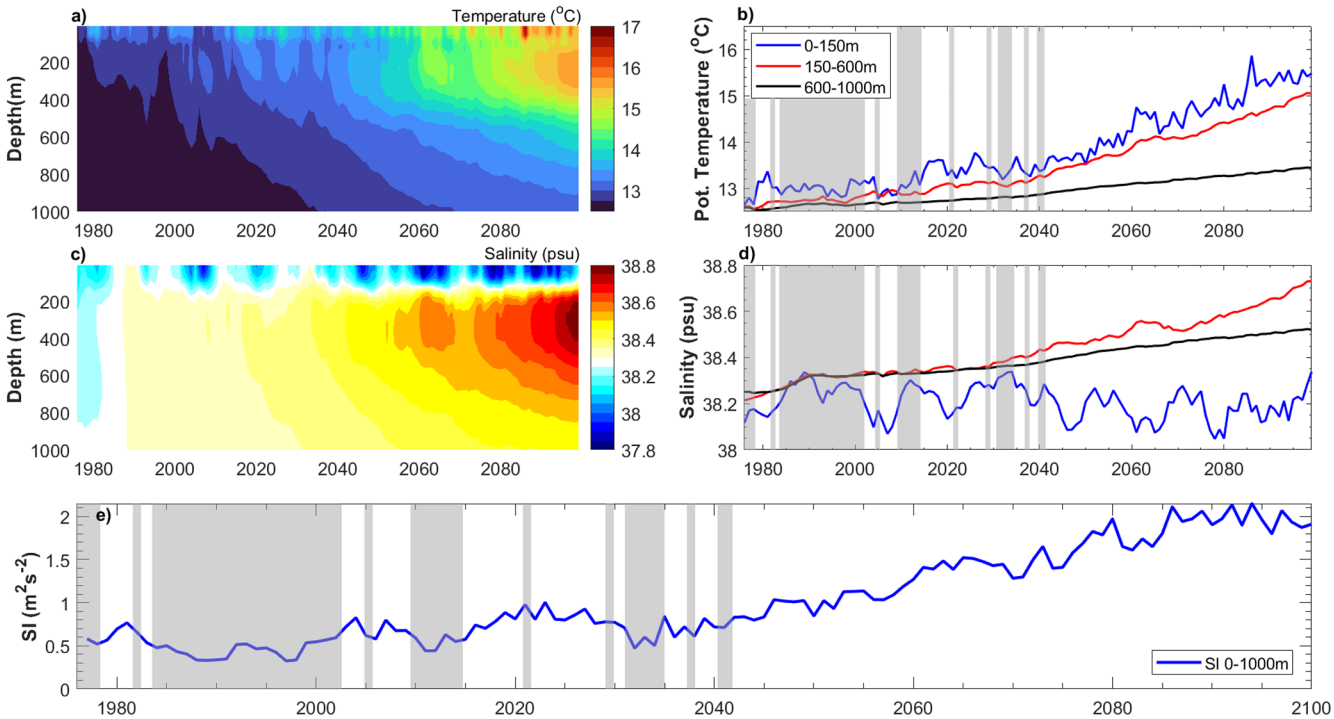

Figure 3. ROM RCP8.5 time series (1976–2099) of 0–1000 m (a) potential temperature (ºC) and (c) salinity (psu). Yearly means of (b) potential temperature (ºC) and (d) salinity (psu) averaged for the layers 0–150 m (blue), 150–600 m (red), 600–1000 m (black). (e) stratification index (SI) for 0–1000 m (blue). All time series correspond to winter months (December-January-February-March) whereas SI was computed in December of preceding year in the Gulf of Lions area. Gray bars indicate Deep water formation episodes (MLD_{max} > 1000 m).

SI gradually increases (0.02 $m^2s^{-2}y^{-1}$) reaching values up to 2.1 m^2s^{-2} at the end of the 21st century. Therefore, the climate change signal introduced by RCP8.5 leads to a higher stratification of the water column, which may hamper the DWF.

In order to assess the relative contribution of LIW and MAW to the deep water formation collapse we compare the SI calculated from spatially and temporally averaged vertical profiles in the GoL in four cases (Figure S3 and Table S2 in Supporting Information S1): (a) using the values corresponding to the pre-collapse period (2006–2041); (b) using the values corresponding to the post-collapse period (2070–2099); and creating additionally two synthetic profiles, (c) one containing the pre-collapse characteristics of MAW (0–150 m depth) with the post-collapse properties of deeper layers (150–1000 m depth; Figure S3g in Supporting Information S1), and (d) a second one with the post-collapse MAW and pre-collapse deeper layers. There is a clear increase in the post-collapse SI with larger SI for the (d) situation (1.35 m^2s^{-2}, Figure S3h in Supporting Information S1) than for the (c; 1.18 m^2s^{-2}, Figure S3g in Supporting Information S1). This suggest that the change in MAW properties causes the 57.8% of the total SI future change while the contribution of LIW is about 42.2% (Table S2 in Supporting Information S1). An analogous analysis is made for assessing the temperature and salinity change contribution, showing that in MAW both are important, but in LIW the contribution of temperature overwhelms salinity (Table S3 in Supporting Information S1).

3.4. Fluxes at the Strait of Gibraltar

The simulated water, heat and salt exchange flows through the SoG are summarized in Table 1. During 2070–2099 (period without DWF) the inflow slightly reduces and the outflow decreases by 0.03 Sv in comparison with 1976–2005 (period with DWF events). The net water flow nearly doubles, increasing by 0.03 Sv, in order to compensate the larger net evaporation over the Mediterraneran basin in the 2070–2099 period. The Mediterranean Outflow (MO) becomes warmer toward the end of the century: The MO warms up from 13.2°C (1976–2005) to 15.2°C (2070–2099). Remarkably, until 2041 the MO temperature does not present any significant change, and from then on it experiences a sharp increase (0.034ºCyr^{-1}, Figure S4 in Supporting Information S1). As a result

Table 1
Mean Water, Heat and Salt Exchange Fluxes, Temperature and Salinity of Inflow and Outflow Waters at SoG for 2006–2041 and 2070–2099 Periods Simulated by ROM Under the RCP8.5 Scenario

	1976–2005	2070–2099	Trend 1976–2099
Water inflow (Sv)	0.538	0.532	$-5.3 \cdot 10^{-5}$ Sv yr^{-1}
Water outflow (Sv)	0.510	0.476	$-3.4 \cdot 10^{-4}$ Sv yr^{-1}
Net water flow (Sv)	$2.8 \cdot 10^{-2}$	$5.6 \cdot 10^{-2}$	$2.9 \cdot 10^{-4}$ Sv yr^{-1}
Heat influx (W)	$2.97 \cdot 10^{13}$	$3.20 \cdot 10^{13}$	$2.1 \cdot 10^{10}$ W yr^{-1}
Heat outflux (W)	$2.56 \cdot 10^{13}$	$2.88 \cdot 10^{13}$	$3.2 \cdot 10^{10}$ W yr^{-1}
Net heat transport (W)	$4.1 \cdot 10^{12}$	$3.2 \cdot 10^{12}$	$-1.1 \cdot 10^{10}$ W yr^{-1}
Salt influx (kg s^{-1})	$1.70 \cdot 10^{7}$	$1.65 \cdot 10^{7}$	$-5.5 \cdot 10^{3}$ kg s^{-1} yr^{-1}
Salt outflux (kg s^{-1})	$1.80 \cdot 10^{7}$	$1.72 \cdot 10^{7}$	$-7.4 \cdot 10^{3}$ kg s^{-1} yr^{-1}
Net salt transport (kg s^{-1})	$-1.0 \cdot 10^{6}$	$-7.0 \cdot 10^{5}$	$1.9 \cdot 10^{3}$ kg s^{-1} yr^{-1}
Temperature of inflow waters (ºC)	16.0	16.3	$2.8 \cdot 10^{-3}$ ºC yr^{-1}
Temperature of outflow waters (ºC)	13.2	15.2	$2.1 \cdot 10^{-2}$ ºC yr^{-1}
Salinity of inflow waters (psu)	36.6	35.8	$-8.6 \cdot 10^{-3}$ psu yr^{-1}
Salinity of outflow waters (psu)	38.0	38.2	$1.5 \cdot 10^{-3}$ psu yr^{-1}

Note. Trends computed from yearly means during 2006–2099. For the net transport calculation, positive values were assigned to inflows and negative to outflows.

of the MO warming the net heat transport through the SoG decreases ($9.0 \cdot 10^{11}$ Wyr^{-1}). Other Med-CORDEX RCP8.5 runs simulate an increase in water inflow/outflow and net transport, but within a large ensemble spread (Soto-Navarro et al., 2020).

The salinity of the inflow at SoG decreases ($-8.6 \cdot 10^{-3}$ psuyr^{-1}) due to the freshening of the inflowing AW. This fresher AW is the main contributor to the surface freshening in the GoL. The outflow becomes saltier ($1.5 \cdot 10^{-3}$ psuyr^{-1}) because of the salinization of LIW and deeper waters (Figure 3), thus the salt transport to Atlantic Ocean increases (Table 1). Then, the collapse of DWF could be one of the driving factors of the changes in characteristics of fluxes at SoG, which reflects changes in the Mediterranean overturning circulation at large scale. However, these transport estimates through the SoG should be taken with caution as the computations were carried out offline, therefore susceptible to inacuracies (Soto-Navarro et al., 2020).

4. Discussion and Conclusions

The response of the NWMed DWF to climate change has been explored in Soto-Navarro et al. (2020). The authors found in an ensemble of six Regional Climate Models a robust decrease of DWF by the end of the 21st century. However, the mechanisms involved were not revealed. Previous studies (Adloff et al., 2015; Somot et al., 2006; Soto-Navarro et al., 2020; Thorpe & Bigg, 2000) have shown that this decrease is robust across various runs, so taking into account the current limited availability of RCSM for the Mediterranean, we use a single model runs trying to identify in a physically consistent way the causes of this collapse. Therefore, we study these mechanisms in one of the simulations used in Soto-Navarro et al. (2020). Specifically, we analyze the simulation with the RCSM ROM under the RCP8.5 scenario (named AWI25-MPI-8.5, in Soto-Navarro et al., 2020). We are aware that relaying on a single model imposes limitations to the generalization of our results, however we are confident that they are a good basis for exploring these mechanisms using a multi-model ensemble analysis in the near future.

Exploring the possible mechanisms (i.e., air-sea fluxes and ocean preconditioning) that lead to this strong MLD_{max} decrease we find out that the air-sea fluxes do not seem to be responsible for the DWF collapse, as the BL does not change significantly (Figure 2b). Changes in the BL also cannot explain the changes in DWF strength, as strong or weak DWF events can happen with similar BL values.

Our results indicate that the changes in properties of the upper and intermediate water masses determining the ocean preconditioning are key in the DWF collapse. In our simulation, the temperatures of MAW and LIW are projected to increase; in turn, the salinity decreases slightly on the surface, while deeper waters become saltier. As shown previously in Parras-Berrocal et al. (2020), the warming and freshening signal of MAW comes to the GoL from the Eastern Atlantic (which is a common feature among CMIP5 models (Levang & Schmitt, 2020; Soto-Navarro et al., 2020)), while warmer and saltier LIW comes from its formation area in the Eastern Mediterranean. These changes increase the vertical density gradient between the MAW and LIW, strongly reducing the vertical mixing between these water masses. Our results do not show a significant change in atmospheric fluxes, changes in MAW and LIW characteristics play the main role in the DWF collapse in the NWMed, which is supported by the results from a simple linear regression relating the MLD_{max}, BL and SI (Figure S5 in Supporting Information S1). The recent study of Margirier et al. (2020) lends some support to our hypothesis: they found in glider and other platforms profiles collected over 2007–2017 that an abrupt jump of LIW temperature and salinity provoked a strong reduction of vertical mixing in the NWMed in 2014. They concluded that under those conditions, stronger atmospheric forcing is needed to trigger deep convection. Amitai et al. (2021) have also recently demonstrated that LIW characteristics play a key role in enabling or disabling the deep convection in the GoL. In agreement with Margirier et al. (2020) and Amitai et al. (2021), our results indicate that the projected DWF collapse in the 21st century is driven by the change in MAW and LIW characteristics. This collapse of NWMed DWF seems to have an impact on the ventilation and on the thermohaline circulation of the Mediterranean Sea. The net flow through the SoG nearly doubles in order to compensate the increase in net evaporation over the Mediterranean basin in the 2070–2099 period. Moreover, in this RCP8.5 scenario the surface Atlantic jet transports more heat and less salt into the Mediterranean basin, causing the hydrographic changes of surface waters (MAW) in the GoL. At the same time, the LIW salinization and warming contribute to a warmer and saltier MO by the end of the 21st century.

Conflict of Interest

The authors declare that they have no conflict of interest.

Data Availability Statement

The model data are available online (https://doi.org/10.5281/zenodo.5595317).

Acknowledgments
I. M. Parras-Berrocal, O. Álvarez and M. Bruno were supported by the Spanish National Research Plan through project TRUCO (RTI2018-100865-BC22). W. Cabos have been funded by the Spanish Ministry of Science, Innovation and Universities, through grant (CGL2017-89583-R). D. Sein was supported by the Ministry of Science and Higher Education of Russia (0128-2021-0014). This work is part of the Med-CORDEX (www.med-cordex.eu) initiative and HyMex program (www.hymex.org).

References

Adloff, F., Somot, S., Sevault, F., Jordà, G., Aznar, R., Déqué, M., et al. (2015). Mediterranean Sea response to climate change in an ensemble of twenty first century scenarios. *Climate Dynamics*, *45*, 2775–2802. https://doi.org/10.1007/s00382-015-2507-3

Amitai, Y., Ashkenazy, Y., & Gildor, H. (2021). The effect of the source of deep water in the Eastern Mediterranean on Western Mediterranean intermediate and deep water. *Frontiers in Marine Science*, *7*, 615975. https://doi.org/10.3389/fmars.2020.615975

Béthoux, J. P., Durrieu de Madron, X., Nyffeler, F., & Tailliez, D. (2002). Deep water in the western Mediterranean: Peculiar 1999 and 2000 characteristics, shelf formation hypothesis, variability since 1970 and geochemical inferences. *Journal of Marine Systems*, *33–34*, 117–131. https://doi.org/10.1016/S0924-7963(02)00055-6

Béthoux, J. P., & Gentili, B. (1999). Functioning of the Mediterranean Sea: Past and present changes related to freshwater input and climate changes. *Journal of Marine Systems*, *20*, 33–47. https://doi.org/10.1016/S09247963(98)00069-4

Darmaraki, S., Somot, S., Sevault, F., Nabat, P., Cabos Nar- Vaez, W. D., Cavicchia, L., et al. (2019). Future evolution of marine heatwaves in the Mediterranean Sea. *Climate Dynamics*, *53*, 1371–1392. https://doi.org/10.1007/s00382-019-04661-z

D'Ortenzio, F., Iudicone, D., De Boyer Montegut, C., Testor, P., Antoine, D., Marullo, S., et al. (2005). Seasonal variability of the mixed layer depth in the Mediterranean Sea as derived from in situ profiles. *Geophysical Research Letters*, *32*, L12605. https://doi.org/10.1029/2005GL022463

Durrieu de Madron, X., Houpert, L., Puig, P., Sanchez-Vidal, A., Testor, P., Bosse, A., et al. (2013). Interaction of dense shelf water cascading and open-sea convection in the Northwestern Mediterranean during winter 2012. *Geophysical Research Letters*, *40*, 1379–1385. https://doi.org/10.1002/grl.50331

Estournel, C., Testor, P., Taupier-Letage, I., Bouin, M.-N., Coppola, L., Durand, P., et al. (2016). HyMeX-SOP2: The field campaign dedicated to dense water formation in the northwestern Mediterranean. *Oceanography*, *29*(4), 196–206. https://doi.org/10.5670/oceanog.2016.94

Giorgi, F. (2006). Climate change hot-spots. *Geophysical Research Letters*, *33*, L08707. https://doi.org/10.1029/2006GL025734

Hagemann, S., & Dümenil-Gates, L. (1998). *A parameterization of the lateral waterflow for the global scale*, Climate Dynamics, 14, 17–31. https://doi.org/10.1007/s003820050205

Hagemann, S., & Dümenil-Gates, L. (2001). Validation of the hydrological cycle of ECMWF and NCEP reanalysis using the MPI hydrological discharge model. *Journal of Geophysical Research*, *106*, 1503–1510. https://doi.org/10.1029/2000JD900568

Herrmann, M., Sevault, F., Beuvier, J., & Somot, S. (2010). What induced the exceptional 2005 convection event in the northwestern Mediterranean basin? Answers from a modeling study. *Journal of Geophysical Research: Oceans*, *115*(C12). https://doi.org/10.1029/2010JC006162

Hibler, W. D. (1979). A dynamic thermodynamic sea ice model. *Journal of Physical Oceanography*, *9*, 815–846. https://doi.org/10.1175/1520-0485(1979)009<0815:adtsim>2.0.CO;2

Houpert, L., Durrieu de Madron, X., Testor, P., Bosse, A., D'Ortenzio, F., Bouin, M. N., et al. (2016). Observations of open-ocean deep convection in the northwestern Mediterranean Sea: Seasonal and interannual variability of mixing and deep water masses for the 2007-2013 period. *Journal of Geophysical Research: Oceans*, *121*(11), 8139–8171. https://doi.org/10.1002/2016JC011857

IPCC. (2013). In T. F. Stocker, D. Qin, G. K. Plattner, M. Tignor, S. K. Allen, J. Boschung, et al. (Eds.), *Climate change 2013: The physical science basis. Contribution of working group I to the fifth assessment report of the intergovernmental panel on climate change* (pp. 1535). Cambridge University Press.

Jacob, D. (2001). A note to the simulation of the annual and in- terannual variability of the water budget over the Baltic Sea drainage basin. *Meteorology and Atmospheric Physics*, *77*, 61–73. https://doi.org/10.1007/s007030170017

Jungclaus, J. H., Fischer, N., Haak, H., Lohmann, K., Marotzke, J., Matei, D., et al. (2013). Characteristics of the ocean simulations in MPIOM, the ocean component of the MPI-Earth system model. *Journal of Advances in Modelling Earth Systems*, *5*, 422–446. https://doi.org/10.1002/jame.20023

Lascaratos, A., Williams, R., & Tragou, E. (1993). A mixed-layer study of the formation of Levantine Intermediate Water. *Journal of Geophysical Research*, *98*(C8), 14739–14749. https://doi.org/10.1029/93JC00912

Leaman, K., & Schott, F. (1991). Hydrographic structure of the convection regime in the Gulf of Lions: Winter 1987. *Journal of Physical Oceanography*, *21*(4), 575–598. https://doi.org/10.1175/1520-0485(1991)021<0575:hsotcr>2.0.CO;2

Léger, F., Lebeaupin Brossier, C., Giordani, H., Arsouze, T., Beuvier, J., Bouin, M.-N., et al. (2016). Dense water formation in the north- western Mediterranean area during HyMeX-SOP2 in 1/36° ocean simulations: Sensitivity to initial conditions. *Journal of Geophysical Research: Oceans*, *121*(8), 5549–5569. https://doi.org/10.1002/2015JC011542

Levang, S. J., & Schmitt, R. W. (2020). What causes the AMOC to weaken in CMIP5? *Journal of Climate*, *33*(4), 1535–1545. https://doi.org/10.1175/JCLI-D-19-0547.1

Levitus, S., Boyer, T. P., Conkright, M. E., O'Brien, T., Antonov, J., Stephens, C., et al. (1998). World Ocean Database 1998, vol.1, Introduction, NOAA Atlas NESDIS 18, Ocean Climate Laboratory, National Oceanography Data Centre, U.S. Gov. Print. Off.

L'Hévéder, B., Li, L., Sevault, F., & Somot, S. (2013). Interannual variability of deep convection in the northwestern Mediterranean simulated with a coupled AORCM. *Climate Dynamics*, *41*(3–4), 937–960. https://doi.org/10.1007/s00382-012-1527-5

Maier-Reimer, E., Kriest, I., Segschneider, J., & Wetzel, P. (2005). *The HAMburg Ocean Carbon Cycle Model HAMOCC5.1 Technical Description Release 1.1. Ber. Erdsystemforschung*. (Vol. 14). Retrieved From: http://hdl.handle.net/11858/00-001M-0000-0011-FF5C-D

Margirier, F., Testor, P., Heslop, E., Mallil, K., Bosse, A., Houpert, L., et al. (2020). Abrupt warming and salinification of intermediate waters interplays with decline of deep convection in the Northwestern Mediterranean Sea. *Scientific Reports*, *10*, 20923. https://doi.org/10.1038/s41598-020-77859-5

Marshall, J., & Schott, F. (1999). Open-ocean convection: Observations, theory, and models. *Reviews of Geophysics*, *37*(1), 1–64. https://doi.org/10.1029/98RG02739

Marsland, S. J., Haak, H., Jungclaus, J. H., Latif, M., & Roeske, F. (2003). The Max-Planck- Institute global ocean/sea ice model with orthogonal curvilinear coordinates. *Ocean Modelling*, *5*(2), 91–127. https://doi.org/10.1016/S1463-5003(02)00015-X

MEDOC Group. (1970). Observations of formation of deep-water in the Mediterranean Sea. *Nature*, *227*, 1037–1040. https://doi.org/10.1038/2271037a0

Menna, M., & Poulain, P. M. (2010). Mediterranean intermediate circulation estimated from Argo data in 2003–2010. *Ocean Science*, *6*, 331–343. https://doi.org/10.5194/os-6-331-2010

Mertens, C., & Schott, F. (1998). Interannual variability of deep-water formation in the northwestern Mediterranean. *Journal of Physical Oceanography*, *28*, 1410–1423. https://doi.org/10.1175/1520-0485(1998)028<1410:IVODWF>2.0.CO;2

Millot, C. (1999). Circulation in the western Mediterranean Sea. *Journal of Marine Systems*, *20*(1–4), 423–440. https://doi.org/10.1016/S0924-7963(98)00078-5

Millot, C. (2005). Circulation in the Mediterranean Sea: Evidences, debates and unanswered questions. *Scientia Marirna*, *69*, 5–21. https://doi.org/10.3989/scimar.2005.69s15

Millot, C. (2014). Levantine intermediate water characteristics: An astounding general misunderstanding! (addendum). *Scientia Marina*, *78*(2), 165–171. https://doi.org/10.3989/scimar.04045.30H

Parras-Berrocal, I. M., Vazquez, R., Cabos, W., Sein, D., Mañanes, R., Perez-Sanz, J., & Izquierdo, A. (2020). The climate change signal in the Mediterranean Sea in a regionally coupled atmosphere–ocean model. *Ocean Science*, *16*, 743–765. https://doi.org/10.5194/os-16-743-2020

Rechid, D., & Jacob, D. (2006). Influence of monthly varying vegetation on the simulated climate in Europe. *Meteorologische Zeitschrift*, *15*(1), 99–116. https://doi.org/10.1127/0941-2948/2006/0091

Rhein, M. (1995). Deep water formation in western Mediterranean. *Journal of Geophysical Research*, *100-C4*, 6943–6959. https://doi.org/10.1029/94JC03198

Robinson, A., Leslie, W., Theocharis, A., & Lascaratos, A. (2001). *Encyclopedia of ocean sciences*. Academic Press Ltd.

Sánchez-Gómez, E., Somot, S., Josey, S. A., Dubois, C., Elguindi, N., & Déqué, M. (2011). Evaluation of Mediterranean Sea water and heat budgets simulated by an ensemble of high resolution regional climate models. *Climate Dynamics*, *37*, 2067–2086. https://doi.org/10.1007/s00382-011-1012-6

Schott, F., & Leaman, K. D. (1991). Observations with moored acoustic doppler current profilers in the convection regime in the Golfe du Lion. *Journal of Physical Oceanography*, *21*, 558–574. https://doi.org/10.1175/1520-0485(1991)021<0558:owmadc>2.0.CO;2

Sein, D. V., Mikolajewicz, U., Gröger, M., Fast, I., Cabos, W., Pinto, J. G., et al. (2015). Regionally coupled atmosphere-ocean- sea ice-marine biogeochemistry model ROM: 1. Description and validation. *Journal of Advance in Modelling Earth Systems*, *7*(1), 268–304. https://doi.org/10.1002/2014MS000357

Seyfried, L., Marsaleix, P., Richard, E., & Estournel, C. (2017). Modelling deep-water formation in The North-west Mediterranean Sea with a new air–sea coupled model: Sensitivity to turbulent flux parameterizations. *Ocean Science*, *13*, 1093–1112. https://doi.org/10.5194/os-13-1093-2017

Somot, S., Houpert, L., Sevault, F., Testor, P., Bosse, A., Taupier-Letage, I., et al. (2018). Characterizing, modelling and understanding the climate variability of the deep water formation in the north-western Mediterranean Sea. *Climate Dynamics*, *51*, 1179–1210. https://doi.org/10.1007/s00382-016-3295-0

Somot, S., Sevault, F., & Déqué, M. (2006). Transient climate change scenario simulation of the Mediterranean Sea for the 21st century using a high-resolution ocean circulation model. *Climate Dynamics*, *27*, 851–879. https://doi.org/10.1007/s00382-006-0167-z

Somot, S., Sevault, F., Déqué, M., & Crépon, M. (2008). 21st century climate change scenario for the Mediterranean using a coupled atmosphere–ocean regional climate model. *Global and Planetary Change*, *63*, 112–126. https://doi.org/10.1016/j.gloplacha.2007.10.003

Soto-Navarro, J., Jordá, G., Amores, A., Cabos, W., Somot, S., Sevault, F., et al. (2020). Evolution of Mediterranean Sea water properties under climate change scenarios in the Med-CORDEX ensemble. *Climate Dynamics*, *54*, 2135–2165. https://doi.org/10.1007/s00382-019-05105-4

Testor, P., Bosse, A., Houpert, L., Margirier, F., Mortier, L., Lego, H., et al. (2018). Multiscale observations of deep convection in the northwestern Mediterranean Sea during winter 2012-2013 using multiple platforms. *Journal of Geophysical Research: Oceans*, *123*, 1745–1776. https://doi.org/10.1002/2016JC012671

Thorpe, R. B., & Bigg, G. R. (2000). Modelling the sensitivity of Mediterranean outflow to anthropogenically forced climate change. *Climate Dynamics*, *16*(5), 355–368. https://doi.org/10.1007/s003820050333

Turner, J. (1973). *Buoyancy effects in fluids: Cambridge monographs on mechanics and applied mathematics*. Cambridge University Press.

Valcke, S. (2013). The OASIS3 coupler: A European climate modelling community software. *Geoscientific Model Development*, *6*, 373–388. https://doi.org/10.5194/gmd-6-373-2013

Vargas-Yáñez, M., Zunino, P., Schroeder, K., López-Jurado, J. L., Plaza, F., Serra, M., et al. (2012). Extreme western intermediate water formation in winter 2010. *Journal of Marines Systems*, *105–108*, 52–59. https://doi.org/10.1016/j.jmarsys.2012.05.010

Waldman, R., Somot, S., Herrmann, M., Bosse, A., Caniaux, G., Estournel, C., et al. (2017). Modelling the intense 2012–2013 dense water formation event in the northwestern Mediterranean Sea: Evaluation with an ensemble a simulation approach. *Journal of Geophysical Research: Oceans*, *122*, 1297–1324. https://doi.org/10.1002/2016JC012437

Waldman, R., Somot, S., Herrmann, M., Sevault, F., & Isachsen, P. E. (2018). On the chaotic variability of deep convection in the Mediterranean Sea. *Geophysical Research Letters*, *45*, 2433–2443. https://doi.org/10.1002/2017GL076319

Wetzel, P., Haak, H., Jungclaus, J., & Maier-Reimer, E. (2004). *The Max-Planck-institute global ocean/sea ice model*. Model MPI-OM Technical report. Retrieved From http://www.mpimet.mpg.de/fileadmin/models/MPIOM/DRAFT_MPIOM_TECHNICAL_REPORT.pdf